

10,11

# Two-dimensional Labbe–Friedel model for interacting carbon chains in a free state and formed on transition metals and their oxides: special features of thermoelectrical characteristics

© S.Yu. Davydov

Ioffe Institute,  
St. Petersburg, Russia

E-mail: sergei.davydov@mail.ru

Received October 21, 2025

Revised January 19, 2026

Accepted January 21, 2026

Within the framework of the tight binding theory, a free rectangular lattice (FRL) formed by orthogonal chains of carbon atoms (a two-dimensional version of the Labbe-Friedel model) is considered, for which analytical expressions for the density of states and estimates of the features of thermoelectric characteristics are obtained. The question of how the obtained results are affected by sub-strates, which are transition metals and their oxides, is discussed. Estimates of charge transfer between the epitaxial rectangular lattice (ERL) and substrates are presented. The influence of indirect interaction of parallel chains and Coulomb interaction of carbon adatoms in a chain on the properties of ERL is considered; the possibility of occurrence of charge and spin density waves is shown.

**Keywords:** rectangular lattice of carbon atoms, direct and indirect interactions of carbon chains, thermoelectric characteristics, ferromagnetic and antiferromagnetic coupling of parallel chains.

DOI: 10.61011/PSS.2026.02.63388.287-25

## 1. Introduction

Papers [1,2] outlined the option of getting the carbon atoms chains adsorbed on the grooved faces of transition metals (TM) and their oxides (TMO — transition metal oxides), or the epitaxial carbynes (epicarbynes). In this case, epicarbynes were considered as isolated chains that do not interact with each other. It is clear, however, that such a situation can occur only at low values of TM and TMO surfaces coverages with carbon adatoms, i.e. at low  $\Theta = N/N_{ML}$ , where  $N$  is the concentration of adatoms and  $N_{ML}$  the concentration of adatoms in a monolayer. With intermediate and high coatings  $\Theta \sim 1$ , two-dimensional (2D) regions — islands will appear on the faces of TM and TMO. As an example of such structures in this paper, we consider rectangular lattices (RL), the length of the short side of which  $a_x$  is equal to the interatomic distance in carbyne (elongated along the axis  $\hat{x}$ ), and the lengths of the sides  $a_y$  range from  $a_x$  (square lattice) to infinity (insulated carbyne). This structure is a two-dimensional analogue of Labbe-Friedel model, first proposed for 3D compounds A-15 [3–5], which in the past were considered promising candidates for the role of high-temperature superconductors<sup>1</sup>. Here we get analytical expressions for the electronic and thermoelectric

<sup>1</sup> Compounds A-15 have the chemical formula  $A_3B$ . A specific feature of the structure of these compounds is that their atoms form a family of linear chains intersecting at right angles with the distance between the atoms in the chain less than the inter-chain distances. The most well studied material A-15 is  $V_3Ga$ . Thus, 3D lattice of A atoms is built into the matrix formed by B atoms. Similarly, the confined carbon chains are not free, but are formed on the facets of TM and TMO which entitles to speak of 2D Labbe-Friedel model.

characteristics of free RL, or FRL (sec. 2), and in sec. 3 the changes made to these characteristics by TM and TMO substrates are discussed. Section 4 outlines the role of indirect exchange for epitaxial RL, or ERL, and in section 5 describes the consequences for FRL and ERL if Coulomb interaction is taken into account.

## 2. Free rectangular lattice

### 2.1. Electronic states

Let's consider the free rectangular lattice (FRL), the law of electron dispersion in the tight-binding approximation has the form

$$E(k_x, k_y) = E_0 + 2t_x \cos(a_x k_x) + 2t_y \cos(a_y k_y),$$

$$|k_{x(y)}| \leq \pi/a_{x(y)}, \quad (1)$$

where  $t_{x(y)}$  is an electron hopping energy between the nearest neighbors along  $\hat{x}(\hat{y})$  axis,  $\mathbf{k} = (k_x, k_y)$  is a 2D wave vector,  $E_0$  is an energy of band center which further will be considered as zero, allowed state bandwidth  $W = 4(t_x + t_y)$ . For the first time, the electronic characteristics of FRL in the tight-binding approximation were considered in [6]. Here, for the same purposes, we use the approach of [7] and obtain the results in a form convenient for further use in this study.

Green's function  $g(k_x, k_y)$  equivalent to the spectrum (1) is

$$g^{-1}(\omega, k_x, k_y) = \omega - E(k_x, k_y) + i0^+, \quad (2)$$

where  $\omega$  is an energy variable. Since  $a_y > a_x = a$ , let's assume  $t_x = t$  and  $t_y = \tau t$ , where  $\tau < 1$ . At

$\tau = 0$  we have a monoatomic chain (or, in case of carbon atoms, cumulene [1,6]), at  $\tau = 1$  we have a square lattice (SL). Next, we will need Green's function  $g(\omega, \tau) = S \int_{\text{BZ}} g(k_x, k_y) dk_x dk_y$  where  $S = a_x a_y$  — area of a unit cell and the integration covers the FRL Brillouin zone. The energy density of states  $\rho(\omega, \tau) = -\pi^{-1} \text{Im} g(\omega + i0^+, \tau)$  for 1D lattice ( $\tau = 0$ ) is equal

$$\rho_{1D}(\varepsilon) = \frac{1}{2\pi t \sqrt{1 - \varepsilon^2}}, \quad (3)$$

where  $\varepsilon = \omega/2t$  [1]; as stated in [7], the density of states of a square lattice ( $\tau = 1$ ) is

$$\rho_{\text{SL}}(\varepsilon) = \frac{1}{2\pi^2 t} K(\kappa), \quad \kappa = \sqrt{1 - \varepsilon^2/4}, \quad (4)$$

where  $K(\dots)$  is a complete elliptic integral of the first kind, [8,9]. Graphs of functions (3) and (4) are given in Figure *a*. Using the scheme from [7] for the law of dispersion (1), it is easy to show that the corresponding Green's function in the energy representation is

$$g(\varepsilon, \tau) = \frac{1}{2\pi t} \frac{2}{\sqrt{\varepsilon^2 - (1 - \tau)^2}} K(\kappa),$$

$$\kappa = \sqrt{\frac{4\tau}{\varepsilon^2 - (1 - \tau)^2}}, \quad (5)$$

and total density of states

$$\rho_{\text{FRL}}(\varepsilon, \tau) = -\frac{1}{\pi^2 t} \times \text{Im} \left[ \frac{1}{\sqrt{\varepsilon^2 - (1 - \tau)^2}} K \left( \sqrt{\frac{4\tau}{\varepsilon^2 - (1 - \tau)^2}} \right) \right] \quad (6)$$

is different from zero only within  $|\varepsilon| \leq (1 + \tau)$ . Since  $K(1/\kappa) = iK(\kappa')$ , at  $(1 - \tau) \leq |\varepsilon| \leq (1 + \tau)$  we have

$$\rho_{\text{FRL}}(\varepsilon, \tau) = \frac{1}{2\pi^2 t} \frac{1}{\sqrt{\varepsilon^2 - (1 - \tau)^2}} K \left( \sqrt{\frac{(1 + \tau)^2 - \varepsilon^2}{4\tau}} \right). \quad (7)$$

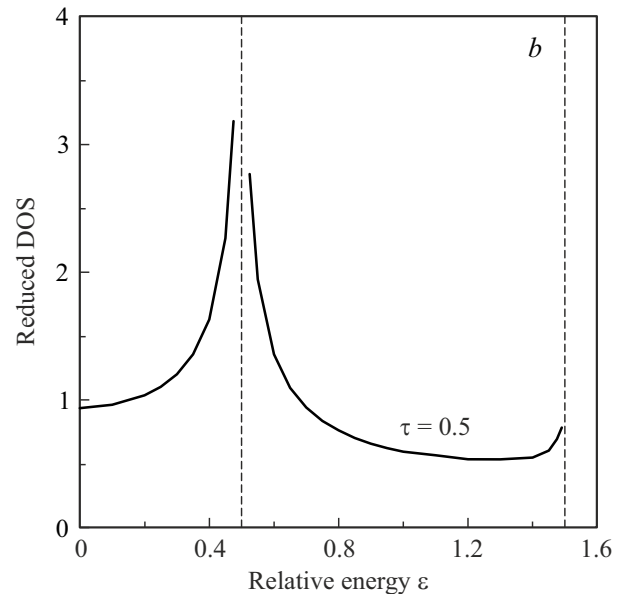
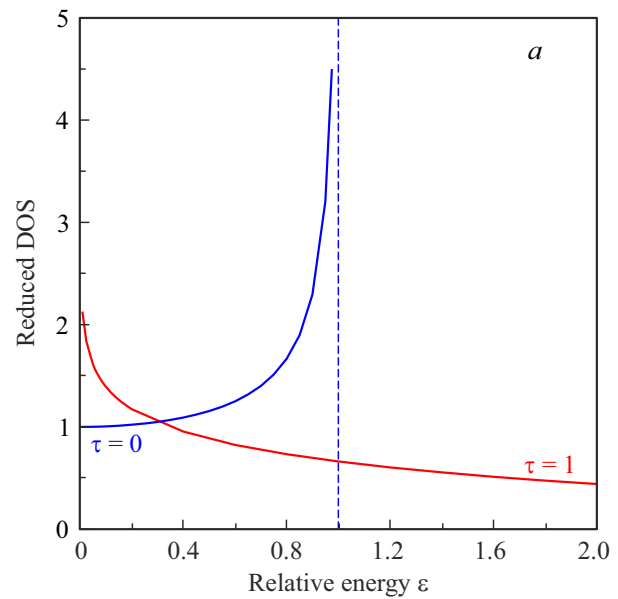
When  $\varepsilon^2 < (1 - \tau)^2$ ,  $\tau \neq 1$ , we get the Green's function as

$$g(\varepsilon, \tau) = \frac{1}{2\pi t} \frac{1}{i\sqrt{(1 - \tau)^2 - \varepsilon^2}} K \left( i\sqrt{\frac{(1 - \tau)^2 - \varepsilon^2}{4\tau}} \right). \quad (8)$$

When comparing the figures *a* and *b* we may see that when moving from 1D and 2D structures to  $1 < \tau < 2$  the density of states for Labbe–Friedel lattice  $|\varepsilon| < 0.5$  has a density of states equivalent to 1D structure, and when  $0.5 < |\varepsilon| < 1.5$  has a to the density of states of a 2D lattice. A more detailed discussion of this transition is given [4].

## 2.2. Specifics of the thermoelectric characteristics

In [10], using the example of a gapped graphene, it was demonstrated for the first time that any drastic changes



Dependence on dimensionless energy  $\varepsilon = \omega/2t$  of the reduced densities of states  $\rho^*(\varepsilon) = \rho(\varepsilon, \tau) \cdot 2\pi t$ : *a* — one-dimensional chain ( $\tau = 0$ ) and square lattice ( $\tau = 1$ ); *b* — rectangular lattice at ( $\tau = 0.5$ ). Only right part of the even functions  $\rho^*(\varepsilon)$  is shown. Dotted line shows the asymptotes.

in the density of states during transition from the regions of the continuous spectrum to the region of the energy gap manifest themselves as specific dependences of its thermoelectric characteristics on energy. For carbynes we studied this effect in papers [1,2]. Based on the kinetic Boltzmann equation in the relaxation time approximation  $\tau_{\text{rel}}$ , we obtain the expression for the diffusive spectral conductivity

$$\sigma(\mu) = e^2 = \rho(\mu) v^2(\mu) \tau_{\text{rel}}(\mu), \quad (9)$$

where  $\mu$  is a chemical potential,  $e$  is an elementary charge,  $v$  is a group velocity of electron.

It is easy to show that for a rectangular lattice  $v^2 = v_x^2 + v_y^2$ , where, according to (1),  $v_{x,y} = -2t_{x,y}a_{x,y} \sin(a_{x,y}k_{x,y})/\hbar$ . Since in Harrison method [11] for the atoms containing only  $s$ - and  $p$ -orbitals, matrix elements of interaction  $t \propto a^{-2}$ , we'll get  $t_x a_x^2 = t_y a_y^2 = |\eta|(\hbar^2/m_e)$ , where  $\hbar$  — reduced Planck constant,  $m_e$  — mass of free electron,  $\eta$  — numerical coefficient determined by the type of hybridization of orbitals and nature of the bond ( $\sigma$  or  $\pi$ ): e.g., for  $sp$ -hybridization and  $\sigma$ -bond the values of  $|\eta|$  are equal 3.19, and for  $\pi$ -bond of  $p$ -orbitals — 0.63. Thus, we have  $m_e v^2 = 4|\eta|t[\sin^2(a_x k_x) + \tau \sin^2(a_y k_y)]$ , so that the average value of the squared velocity in the Brillouin zone is  $\langle v^2 \rangle_{\text{BZ}} \approx 2|\eta|t(1 + \tau)/m_e$ . From here we get,  $v_x^2 = \langle v_x^2 \rangle_{\text{BZ}}/(1 + \tau)$  and  $v_y^2 = \tau \langle v_y^2 \rangle_{\text{BZ}}/(1 + \tau)$ . Since within quadratic approximation of the spectrum (1) in the center of zone  $v^2 \approx 2|\mu|/m_e$ , and at the boundaries of zone  $v^2 \approx [2t(1 + \tau) - \mu]/m_e$ ; at  $\mu = 0$  and  $\mu = \pm 2t(1 + \tau)$ , the velocities  $v_{x,y}$  go to zero.

Let's consider Seebeck coefficient as a thermoelectric (TE) characteristic.

$$S(\mu) = C_S \left( \frac{\partial \ln \sigma(\mu, T=0)}{\partial \mu} \right), \quad C_S = -\pi^2 k_B^2 T / 3e, \quad (10)$$

where  $k_B$  is a Boltzmann constant,  $T$  is a temperature, and TE factor of power  $PF = \sigma S^2$ . If, in accordance with Fermi golden rule, we assume  $\tau_{\text{rel}}(\mu) \propto \rho^{-1}(\mu)$  (the most popular approximation of the relaxation time [1,12]), then instead of (10) we get  $\sigma(\mu) = e^2 v^2(\mu)$ . Then  $S \equiv S_v = v^{-2}(\partial v^2 / \partial \mu)$  and when  $\mu \rightarrow 0$  we have  $|S(\bar{\mu})| \rightarrow |\bar{\mu}|^{-1}$  and  $PF(\bar{\mu}) \rightarrow 0$ ; when  $\bar{\mu} \rightarrow \pm(1 + \tau)$  we have  $|S(\bar{\mu})| \rightarrow |(1 + \tau) - \bar{\mu}|^{-1}$  and  $PF(\bar{\mu}) \rightarrow 0$ , where  $\bar{\mu} = \mu/2t$ .

If we assume the relaxation time  $\tau_{\text{rel}}(\mu) = \text{const}$  [1,2,12], then, we get that  $S \propto (S_v + S_\rho)$ , where, similar as mentioned above,  $S_v = v^{-2}(\partial v^2 / \partial \mu)$  and  $S_\rho = \rho^{-1}(\partial \rho / \partial \mu)$ . Then, at  $\rho_{\text{FRL}}(\bar{\mu}) \propto |\bar{\mu}^2 - (1 - \tau)^2|^{-1/2}$  we have  $S_\rho \propto |\bar{\mu}^2 - (1 - \tau)^2|^{-1}$  and  $PF \propto |\bar{\mu}^2 - (1 - \tau)^2|^{-5/2}$ . Using formula (1), it is easy to show that condition  $\varepsilon_\pm = \pm(1 - \tau)$  is realized, respectively, for the wave vectors ( $k_x = 0, k_y = \pm\pi/a_y$ ) and ( $k_x = \pm\pi/a_x, k_y = 0$ ). Divergences at the boundaries of the continuous spectrum occur at  $\kappa \rightarrow 1$ , when  $\varepsilon_\pm = \pm(1 + \tau)$ , i.e. at the point  $\Gamma(k_x = 0, k_y = 0)$  of the two-dimensional Brillouin zone and at its boundaries ( $k_x = \pm\pi/a_x, k_y = \pm\pi/a_y$ ). In this case, the function  $K(\kappa) \rightarrow \ln(4/\kappa')$ , where  $\kappa' = \sqrt{1 - \kappa^2}$  [8,9], so that  $\kappa' = \sqrt{|\bar{\mu}^2 - (1 + \tau)^2|}/4t$  and the divergence of  $\rho_{\text{FRL}}(\mu)$  is logarithmic (in a square lattice, such a divergence of the density of states occurs in the middle of the band not zone [7]).

It is interesting to note that the dimensionless effective masses of electrons when the electrons move along  $\hat{x}$  and  $\hat{y}$  axes are equal to  $m_x = m_y = m_e/|\eta|$ , which follows exclusively from the scaling of matrix elements  $t \propto a^{-2}$  according to Harrison [11].

### 3. Epitaxial rectangular lattice

In accordance with the adsorption approach to describing the electronic states of epitaxial 2D structures (epilayers) (see [1,2] and the references given there), instead of (2), the Green function of epitaxial RL (ERL) should be introduced:

$$G^{-1}(\omega, k_x, k_y) = g^{-1}(\omega, k_x, k_y) + \Sigma(\omega), \quad (11)$$

where the self-energy part responsible for interaction with the substrate is  $\Sigma(\omega) = \Lambda(\omega) - i\Gamma(\omega)$  and the functions  $\Lambda(\omega)$  and  $\Gamma(\omega)$  describe, respectively, the shift and broadening of the levels of the free structure. In this case,  $\Gamma(\omega) = \pi V^2 \rho_{\text{sub}}(\omega)$ , where  $V$  is the matrix element of the interaction of the epilayer with the substrate characterized by the density of states  $\rho_{\text{sub}}(\omega)$ , and  $\Lambda(\omega) = \pi^{-1} P \int \Gamma(\omega')(\omega - \omega')d\omega'$  and the symbol  $P$  indicates the main value of the integral, which is taken over the entire energy space. Thus, we may assume that expressions (5)–(8) obtained for FRL formally remain in force, but the reduced energy  $\varepsilon$  shall be replaced by  $\varepsilon - \lambda(\varepsilon) + i\gamma(\varepsilon)$ , where  $\lambda(\varepsilon) = \Lambda(\varepsilon)/2t$  and  $\gamma(\varepsilon) = \Gamma(\varepsilon)/2t$ . Despite the apparent simplicity of such a substitution, it greatly complicates the final analytical results. Since in this paper we strive only for qualitative estimates (since there is nothing to compare the quantitative results with, anyway), here, as in the studies [1,2], we will use rather radical simplifications.

#### 3.1. TM substrate

The adsorption properties of  $d$  metals, including their grooved faces, have been known for a long time (see the relevant information in [1]). Considering the non-magnetic TM, let's assume  $\rho_{\text{sub}}(\omega)$  as

$$\rho_{\text{TM}}(\Omega_d) = \begin{cases} \rho_d, & |\Omega_d| \leq W_d/2, \\ 0, & |\Omega_d| > W_d/2. \end{cases} \quad (12)$$

Here  $\Omega_d = \omega - E_d$ ,  $\rho_d = \text{const}$ ,  $E_d$  is an energy of the center of  $d$ -zone with its width equal to  $W_d$  (Friedel model). Then the broadening function  $\Gamma_d(\Omega_d) = \pi V_d^2 \rho_{\text{TM}}(\Omega_d)$ , where  $V_d$  is the matrix element of the interaction of  $d$ -states of TM with rectangular lattice states. The corresponding shift function is

$$\bar{\Gamma}_d(\Omega_d) = \frac{\bar{\Gamma}_d}{\pi} \ln \left| \frac{\Omega_d + W_d/2}{\Omega_d - W_d/2} \right|, \quad (13)$$

where  $\bar{\Gamma}_d = \pi V_d^2 \rho_d$ .

For further analysis, we'll make some simplifications: having in the spectrum of free RL the four singular points  $\varepsilon_{1\pm}$  and  $\varepsilon_{2\pm}$  (Figure *b*), we represent the approximate density of states as

$$\rho_{\text{FRL}}^{\text{ap}}(\varepsilon, \tau) = \frac{1}{2} \sum_{i=1,2; s=\pm} \delta(\varepsilon - \varepsilon_{is}),$$

$$\varepsilon_{1\pm} = \pm(1 + \tau) \text{ and } \varepsilon_{2\pm} = \pm(1 - \tau), \quad (14)$$

where  $\delta(\dots)$  — Dirac delta function. The density of states of the epitaxial ERL will be written as

$$\rho_{\text{ERL}}^{\text{ap}}(\varepsilon, \tau) = -\frac{1}{2} \sum_{i=1,2; s=\pm} f_{is}(\varepsilon)_i, \quad (15)$$

$$f_{is}(\varepsilon) = \frac{1}{\pi} \frac{\bar{\gamma}_d}{[\varepsilon - \varepsilon_{is} - \lambda(\varepsilon)]^2 + \bar{\gamma}_d^2},$$

where  $\bar{\gamma}_d = \bar{\Gamma}_d/2t$ , „ap“ for the densities of states (14) and (15) indicate their approximation nature.

Let us proceed to numerical estimates. As illustrated in [13], for  $\pi$ -interaction of  $p$ -orbitals  $t \sim 3$  eV, thus,  $W = 4t(1 + \tau) \sim 18$  eV when  $\tau = 0.5$ . For TM in the mid  $4d$ - and  $5d$ -series  $W_d \sim 10$  eV [14]. For the grooved faces of (112) molybdenum and tungsten, the work functions are within  $\varphi_d \sim 4.4$ – $4.7$  eV, which is close to the work functions of carbon structures  $\varphi_C \sim 4.5$  eV (see [1]). Therefore, in the future we will be interested in a relatively narrow energy range  $|\omega| \leq 1.5$  eV, i.e.  $|\varepsilon|, |\mu| \leq 0.25$ . In this case, the zones of allowed states of the carbon structure and TM substrate can be considered infinitely wide, which means that  $\Lambda(\omega) = 0$  [15] and in (15) it is necessary to assume  $\lambda(\varepsilon) = 0$ . Then, ERL occupation numbers are equal

$$\tilde{n}_{\text{ERL}}^{\text{ap}} = \frac{1}{2} \sum_{i=1,2; s=\pm} F(\varepsilon_{is}), \quad F(\varepsilon_{is}) = \frac{1}{\pi} \operatorname{arccot} \frac{\varepsilon_{is} - \mu}{\bar{\gamma}_d}. \quad (16)$$

It is easy to see that for  $\mu = 0$  from (16) we get  $\tilde{n}_{\text{ERL}}^{\text{ap}} = 1$ , the tilde in (16) and further refers to the characteristics of epitaxial structures.

Let's introduce the parameter  $v_{\text{ERL}}^{\text{ap}} = \partial \tilde{n}_{\text{ERL}}^{\text{ap}} / \partial \tau$ , which determines the dependence of the approximate occupation numbers on the constant of interchain interaction  $\tau$ . Since the value  $\tau$  is proportional to the degree of surface coverage by  $\Theta$  atoms, the parameter  $\tilde{v}_{\text{ERL}}^{\text{ap}}$  characterizes the concentration dependences of the occupation numbers of  $\tilde{n}_{\text{ERL}}$  atoms and their charges  $\tilde{Z}_{\text{ERL}} = 1 - \tilde{n}_{\text{ERL}}$ , which is a classic problem physics of adsorption [16,17]. It is easy to demonstrate that

$$\tilde{v}_{\text{ERL}}^{\text{ap}} = -\frac{1}{2} \sum_{i=1,2; s=\pm} f_{is}(\mu) \left( \frac{\partial \varepsilon_{is}}{\partial \tau} \right), \quad (17)$$

$$\partial \varepsilon_{1\pm} / \partial \tau = -\partial \varepsilon_{2\pm} / \partial \tau = \pm 1,$$

where in the functions  $f_{is}(\mu)$  we need to assume  $\lambda(\varepsilon) = 0$ . Obviously, when  $\mu = 0$  we'll get  $\tilde{v}_{\text{ERL}}^{\text{ap}} = 0$ . It should be noted that according to  $\bar{\Gamma}_d \sim 1$  eV [1], i.e.  $\bar{\gamma}_d \approx 0.17$  and, as shown above,  $|\mu| < 0.25$ . When  $|\mu| \ll (1 \pm \tau)$  we obtain  $f_{is} \sim \bar{\gamma}_d / \pi (1 \pm \tau)^2$ . From the point of view of dependencies  $\tau(\Theta)$ , the region  $|\mu| \sim 1 - \tau$  is of the greatest interest. The obtained ratios are consistent with a well-known experimental fact: with the growth of  $\mu$ , the levels occupation with energy less than  $\mu$  rises, and with the energy more than  $\mu$  — declines [18,19]. The case of small  $|\mu|$  is interesting primarily because the carbon atoms remain practically neutral, i.e. they retain the same state as in the free structure.

In conclusion, we note that in case of a TM substrate, the divergences of TE characteristics discussed in sec. 2, disappear turning into corresponding extremums. The interest in the extreme values of Seebeck coefficient and TE power factor is due to the search for materials and heterostructures for which  $PF > 1$ .

### 3.2. TMO substrate

The problem of one-dimensional carbon structures on the grooved faces of transition metal oxides was considered in [1]. At that, parallel faces form chains of  $d$  metals and oxygen atoms (see, for example, the structures of rutile (001) and wurtzite (10 $\bar{1}$ 0) and (11 $\bar{2}$ 0); note also that grooved faces are characteristic not only for TMO, but also for  $sp$  metal oxides: e.g., the face (100) of the rock salt lattice (CaO and MgO) [20,21].

The valence band of TMO is known to be formed mainly by  $p$ -states of oxygen, and the conduction band contains  $d$ - and valence  $s$ -states of transition metal atoms [1]. Now we need to find the functions  $\Lambda(\omega)$  and  $\Gamma(\omega)$ . In the study [1], the densities of states of the valence band (V) and the conduction band (C) were described by the Friedel model (12):  $\rho_{V(C)}(\Omega_{V(C)})$ , where  $\Omega_{V(C)} = \omega - E_{V(C)}$  and bandwidths are equal  $W_{V(C)}$ . However, it is possible to further simplify the task and use Haldane-Anderson model of the density of states [18,19,22]:

$$\rho_{\text{TMO}}(\Omega) = \begin{cases} \bar{\rho}, & |\Omega| \geq E_g/2, \\ 0, & |\Omega| < E_g/2. \end{cases} \quad (18)$$

Here  $\bar{\rho} = \text{const}$ ,  $\Omega = \omega - E_0$ ,  $E_0$  is an energy of the center of the band gap which is  $E_g$  wide. Then the broadening of RL states is  $\bar{\Gamma} = \pi \bar{V}^2 \bar{\rho}$ , where  $\bar{V}$  is a matrix element for describing the interaction of  $p$ -states of carbon with  $d$ -states of the substrate, and their shift is

$$\Lambda(\Omega) = \frac{\bar{\Gamma}}{\pi} \ln \left| \frac{\Omega - E_g/2}{\Omega + E_g/2} \right|. \quad (19)$$

The graph of the function (19) is shown in Figures 4 and 8.4 in [18,19]: its comparison with the graph of the total shift function for TMO substrate  $\Lambda(\omega) = \Lambda_V(\omega) + \Lambda_C(\omega)$  (Figure 1 in [1]), confirms their qualitative compliance. Note that expressions (18) and (19) are well suited to the description of  $4d$ - and  $5d$ -metal oxides characterized by fairly wide  $d$ -zones, whereas Friedel's model better describes the oxides of  $3d$ -metals with narrow  $d$ -zones. However, if we take into account the presence of valence  $s$ -states [23], then the conduction band can be considered, as in (18), — a semi-infinite band. Such simplifications are quite appropriate, as we strive to obtain only high-quality results. Now, as in the case of TM substrate, we use an approximation of (15). Here, however, we cannot a priori assume  $\Lambda(\omega) = \lambda(\omega) = 0$ , since there is a band gap in the spectrum. However, if specific points  $\varepsilon_{1\pm}$  and  $\varepsilon_{2\pm}$  (Figure b) fall within the region  $\bar{\rho} = \text{const}$

and are more than a few  $\bar{p}$  away from the edges of the band gap, then  $\lambda(\omega) = 0$  and all the calculations in the previous section may be considered as valid. If any of the specific points falls into the band gap, then there is no broadening of the corresponding level, and its shift is  $\lambda(\omega) \neq 0$ . The estimates of the TMO based epilayers are somewhat complicated because of the lack of data on the work functions of  $\varphi_{\text{TMO}}$  oxides (thus, for instance, in the monography [20] and review [21] there are no any  $\varphi_{\text{TMO}}$  values provided at all). The reasons for this situation are explained in [24–27] and are mainly reduced to the nonstoichiometry of TMO (oxygen deficiency) and the degree of cation oxidation.

Note that, despite the use of the semiconductor model of the density of states (15), from the standard band theory standpoint, most TMO with partially occupied  $d$ -bands are metals, which is true for the most of  $4d$ - and  $5d$ -compounds. The same is true for the series of  $3d$ -oxides (e.g.,  $\text{Ti}_2\text{O}$ ,  $\text{Fe}_3\text{O}_4$  and  $\text{VO}_2$ ). However, in the case of narrow  $d$ -bands ( $\text{MnO}$ ,  $\text{CoO}$ ,  $\text{NiO}$ ,  $\text{CuO}$ ) due to Coulomb repulsion of  $d$ -electrons (Hubbard repulsion), we have an insulator.

#### 4. Accounting of the indirect interaction of carbon adatoms in ERL

In the formulation of Labbe-Friedel model for FRL in sec. 2 we believed that both the interatomic interaction in the chain and the interchain interaction are direct or kinetic exchange of electrons through overlapping orbitals of the nearest neighbors and are described by the matrix elements  $t_x$  and  $t_y$ . In the initial version of [4,5] model, this approach is natural, since in A-15 couplings, the distance between the nearest neighbors in the chain  $a_x$  is only 22% less than the interchain distance  $a_y$ . However, if  $a_y \gg a_x$ , then we should talk about an indirect or implied inter-chain exchange through the electronic states of the substrate [15,17,19]. Using the data from [28–30], for ERL formed on TM and TMO substrates the matrix elements  $t_{x,y}$ , may be represented as

$$t_{x,y}^{\text{ind}} \propto \frac{V_{\text{C/sub}}^2}{W_d} \frac{\sin(q_{x,y}^* a_{x,y}/2)}{(q_{x,y}^* a_{x,y}/2)}, \quad (20)$$

where  $V_{\text{C/sub}}$  is a matrix element (averaged over the substrate's Brillouin zone) of interaction of  $p$ -states of carbon atoms with  $d$ -band of the substrate,  $W_d$  is a width of  $d$ -bands in TM or TMO,  $q_{x,y}^*$  — wave vector of truncation. Such interaction is an equivalent of RKKY-interaction (RKKY — Ruderman–Kittel–Kosuya–Yosida) [15–17]. Despite the alternating nature, indirect exchange can lead to the appearance of regular structures: an example of this is the lattices formed by positively charged adatoms of alkaline and alkaline-earth metals [16,17].

As a simple example of the implied interaction effect on the phonon spectrum of an epistructure, consider the bond stretching vibrations of a FRL lattice with longitudinal

acoustic frequencies  $\bar{\omega}_{x,y}$  equal to

$$M\bar{\omega}_{x,y}(q_{x,y}) = 4\alpha_{x,y} \sin^2(q_{x,y} a_{x,y}/2),$$

$$|q_{x,y}| \leq \pi/a_{x,y}, \quad (21)$$

where the force constants of central interaction of  $\alpha_{x,y} = 4t_{x,y}/a_{x,y}^2$ ,  $q_{x,y}$  are the frequencies of longitudinal phonons,  $M$  is a mass of the carbon atom [13]. Thus,  $\alpha_x/\alpha_y = \tau(a_y/a_x)^2 = (a_y/a_x)^4$ . According to [13] for the cumulene we have  $\alpha_x = 36 \text{ eV/\AA}^2$ ,  $\bar{\omega}_x(\pi/a_x) \approx 1800 \text{ cm}^{-1}$ . In accordance with the data from [28–30] in case of ERL, the matrix elements  $t_{x,y}$  should be replaced with  $\bar{t}_{x,y} = |t_{x,y} + t_{(,y)}^{\text{ind}}|$ . Then, assuming  $\eta = |t_{x,y}^{\text{ind}}|/t_{x,y} \ll 1$ , we get  $\bar{\alpha}_{x,y} \approx \alpha_{x,y} [1 + \text{sgn}(t_{x,y}^{\text{ind}})\eta]$  and  $\bar{\omega}_{x,y} \approx \bar{\omega}_{x,y} [1 + \text{sgn}(t_{x,y}^{\text{ind}})\eta]$ . The shift of frequencies  $\Delta\bar{\omega}_{x,y} = |\bar{\omega}_{x,y} - \bar{\omega}_{x,y}|$  can be easily detected using spectroscopy methods.

#### 5. Accounting of Coulomb interactions in FRL and ERL

Using the approach from [13], let's consider how the above results are impacted by taking into account the Coulomb repulsion of electrons with opposite spins  $U$  localized on a single carbon atom and also the short-range repulsion of electrons of the nearest neighbors  $G$  in cumulene. According to the study [13], taking into account these interactions in the non-magnetic case results in transition of electrons between the nearest neighbors, so that neighboring atoms 1 and 2 in the chain acquire the occupation numbers  $n_1$  and  $n_2$  and are characterized by energy levels  $E_{1,2} = E_0 + Un_{1,2}/2 + 2Gn_{2,1}$ . For  $U > G \gg t_x$ , for the free carbyne in zero approximation over  $t_x$ , the energy of such a diatomic chain per atom is  $(U - 2G)v^2$ , which means that when  $G > U/4$ , the energy state with  $v \neq 0$  and  $n_{1,2} = 1 \pm v$  is beneficial, which is consistent with the charge density wave (CDW) in the chain (in the absence of any data on carbynes, we'll use data for the free-standing graphene, where, neglecting the shielding by its own electrons  $U = 17.0 \text{ eV}$ ,  $G = 8.5 \text{ eV}$ , taking into account the same  $U = 9.3 \text{ eV}$ ,  $G = 5.5 \text{ eV}$  [31]). Then, dispersion law in the chain will be expressed as

$$E_x^\pm(k_x) = \pm \sqrt{(U/2 - 2G)v^2 + 4t_x^2 \cos^2(k_x a_x)}, \quad (22)$$

where  $v = (n_1 - n_2)/2$ . From a clearly electrostatics standpoint, we may see that charges of opposite signs should be located in the corners of FRL unit cell. Thus, the presence of CDW in the chain can lead to the occurrence of a two-dimensional ionic structure. These structures are only started to be investigated [32–34]

In the case of epicarbyne, which strongly interacts with TM or TMO substrates (when  $\bar{\Gamma}_d \gg t$ ), the condition for the occurrence of CDW is the fulfillment of the inequality  $(2G - U/2) > 2\pi^2 t_x^2 / \bar{\Gamma}_d$  [13]; general case is considered in [32,33].

Now let's consider the situation when the atoms of the chain have an uncompensated spin moment  $m = n_{\sigma} - n_{-\sigma}$ , where the spin index is  $\sigma = (\uparrow, \downarrow)$ , i.e., at  $n_{\uparrow}n_{\downarrow}$ . To determine  $m$ , it is convenient to use Anderson model [15,19,34], according to which the condition  $m \neq 0$  when  $n = 1$  is the validity of inequality  $U/\pi\bar{\Gamma} > 1$  [35]. Therefore, for ERL on TM and TMO two options are envisaged: 1) neighboring chains have the same values  $m$  (ferromagnetic structure of ERL), 2) neighboring chains have opposite values (antiferromagnetic structure of ERL, while we can talk about a spin density wave (SDW) in the direction of  $\hat{y}$ ). The easiest way to assess which case is realized is using the results of [28,36–38]: according to these sources, the sign of the magnetic interaction depends on the relative position of the chemical potential  $\mu$  and the level  $E_0$  of the carbon atom. If  $\mu \sim E_0$  or  $\mu \sim E_0 + U$  and  $U \gg t$ , then the parallel arrangement of the spins is preferred, otherwise the antiferromagnetic state will be considered as a more benign. However, it should be noted that these results were obtained for magnetic impurities in *sp*metals with a density of states  $\rho_{\text{met}} = \text{const}$ .

## 6. Conclusion

So, we have considered a two-dimensional version of Labbe-Friedel model, representing itself an intersecting chains of carbon atoms forming a lattice with a rectangular unit cell. Such a structure is not as academic as it might seem: the work [39] discusses, for example, the reality of a 2D square lattice of polonium, the only metal with its bulky samples having a simple cubic lattice. In general, the interest in 2D metals is steadily growing [40–44]. It is known that the properties of 3D and 2D metals are similar, and the models of their description are identical (see details in [45]). The interest in 2D TMO is also on the rise [46–51]. Therefore, our choice of substrates and the results presented here will probably be useful for the two-dimensional substrates — equivalents of TM and TMO. Note that this paper presents not the results of specific calculations, but general schemes proposed to describe the properties of carbon structures with an increase in the surface concentration of carbon adatoms  $\Theta$ . It seems to us that today it is such schemes that can be useful for understanding the properties of low-dimensional carbon structures formed on TM and TMO.

Finally, it should be noted that the studies [52,53] provided a revised conventional approach to describing the thermoelectric properties [54], in particular, the Mott formula (10), for low-dimensional systems.

## Conflict of interest

The authors declare that they have no conflict of interest.

## References

- [1] S.Yu. Davydov. Phys. Solid State **66**, 701 (2024). DOI: 10.61011/PSS.2024.05.58500.16.
- [2] S.Yu. Davydov. FTT, **67**, 189 (2025) (in Russian).
- [3] J. Labbe. Phys. Rev. **158**, 647 (1967).
- [4] S.V. Vonsovsky, Yu.A. Izyumov, E.Z. Kurmaev. Sverkhprovodimost' perekhodnykh metallov, ikh splavov i soedineniy. Nauka, M. (1977). Ch. 5 (in Russian).
- [5] Problema vysokotemperaturnoy sverkhprovodimosti / Edited by V.L. Ginzburg, D.A. Kirzhnits. Nauka, M. (1977). Ch. 7 (in Russian).
- [6] R. Piasecki. arXiv: 0804.1037.
- [7] E. Kogan, G. Gumbs. arXiv: 2008.05544.
- [8] I.S. Gradshtein, I.M. Ryzhik. Tablitsy integralov, summ, ryadov i proizvedeniy, Nauka, M. (1971) (in Russian).
- [9] E. Janke, F. Emde, F. Lösch. Tafeln Höherer Funktionen. B.G. Teubner, Stuttgart (1960).
- [10] A.A. Varlamov, A.V. Kavokin, I.A. Luk'yanchuk, S.G. Sharapov. Phys.-Uspekhi **55**, 1146 (2012).
- [11] W.A. Harrison. Phys. Rev. B **27**, 3552 (1983).
- [12] S.Yu. Davydov. Phys. Solid State **65**, 1942 (2023).
- [13] S.Yu. Davydov. Semiconductors **53**, 954 (2019).
- [14] V.Yu. Irkhin, Yu.P. Irkhin. arXiv: 9812072.
- [15] C. Kittel. Quantum Theory of Solids. Wiley, N.Y.–London (1963). Ch. 18.
- [16] L.A. Bol'shov, A.P. Napartovich, A.G. Naumovets, A.G. Fedorus. Usp. Fiz. Nauk **122**, 125 (1977).
- [17] O.M. Braun, V.K. Medvedev. Usp. Fiz. Nauk **157**, 631 (1989).
- [18] S.Yu. Davydov, S.V. Troshin. Solid State Phys. **49**, 1508 (2007).
- [19] S.Yu. Davydov, A.A. Lebedev, O.V. Posrednik. Elementarnoye vvedeniye v teoriyu nanosistem „Lan“, SPb (2014). Ch. 8 (in Russian).
- [20] V.E. Henrich, P.A. Cox. The Surface Science of Metal Oxides. Cambridge Univ. Press (1994). Ch. 2.
- [21] H.-J. Freund, H. Kuhlenbeck, V. Staemmler. Rep. Prog. Phys. **59**, 283 (1996).
- [22] F.D.M. Haldane, P.W. Anderson. Phys. Rev. B **6**, 2553 (1976).
- [23] W.A. Harrison. Electronic Structure and the Properties of Solids. W.H. Freeman & Co., San Francisco (1980). Ch. 19.
- [24] M.T. Greiner, L. Chai, M.G. Helander, W.-M. Tang, Z.-H. Lu. Adv. Funct. Mater. **22**, 4557 (2012).
- [25] Z. Zhong, P. Hansmann. Phys. Rev. B **93**, 235116 (2016).
- [26] W. Hayami, S. Tang, T.-W. Chiu, J. Tang. ACS Omega **6**, 14559 (2021).
- [27] K. Cieslik, D. Wrana, M. Rogala, C. Rodenbücher, K. Szot, F. Krok. Crystals **13**, 1052 (2023).
- [28] S. Alexander, P.W. Anderson. Phys. Rev. **133**, A1594 (1966).
- [29] S.Yu. Davydov. Phys. Solid State **66**, 1538 (2024).
- [30] S.Yu. Davydov. Phys. Solid State **54**, 1619 (2012).
- [31] T.O. Wehling, E. Sasioglu, C. Friedrich, A.I. Lichtenstein, M.I. Katsnelson, S. Blügel. Phys. Rev. Lett. **106**, 236805 (2011).
- [32] M. D'Onofrio, Y. Xie, A.J. Rasmusson, E. Wolanski, J. Cui, P. Richerme. Phys. Rev. Lett. **127**, 020503 (2021).
- [33] S. Ono. arXiv: 2203.02122.
- [34] Y.H. Teoh, F. Rajabi, R. Islam. Phys. Rev. A **109**, 032426 (2024).
- [35] S.Yu. Davydov. Phys. Solid State **53**, 1674 (2017).
- [36] T. Morya. Spin Fluctuations in Itinerant Electron Magnetism. Springer, Berlin (1985). Ch. 6.

- [37] S.Yu. Davydov, O.V. Posrednik. Namagnichennost' karbina, sformirovannogo na 3d-magnetikakh. XXIX Symposium, 10–14 March 2025 Nizhniy Novgorod. Theses of Reports, p. 367–368 (in Russian).
- [38] S.Yu. Davydov. Phys. Solid State **67**, 363 (2025).
- [39] S. Ono. Sci. Rep. **10**, 11810 (2020).
- [40] J. Nevalaita, P. Koskinen. Phys. Rev. B **97**, 035411 (2018).
- [41] J. Nevalaita, P. Koskinen. AIP Advances **10**, 065327 (2020).
- [42] T. Wang, M. Park, Q. Yu, J. Zhang, Y. Yang. Mater. Today Adv. **8**, 100092 (2020).
- [43] S. Ono. arXiv: 2007.06774.
- [44] W.X. Zhou, H.J. Wu, J. Zhou, S.W. Zeng, C.J. Li, M.S. Li, R. Guo, J.X. Xiao, Z. Huang, W.M. Lv, K. Han, P. Yang, C.G. Li, Z.S. Lim, H. Wang, Y. Zhang, S.J. Chua, K.Y. Zeng, T. Venkatesan, J.S. Chen, Y.P. Feng, S.J. Pennycook, A. Ariando. Commun. Phys. **2**, 125 (2019).
- [45] S.Yu. Davydov, O.V. Posrednik. Semiconductors **57**, 731 (2023).
- [46] K. Kalantar-zadeh, J.Z. Ou, T. Daeneke, A. Mitchell, T. Sasaki, M.S. Fuhrer. Appl. Mater. Today **8**, 73 (2016).
- [47] T. Yang, T.T. Song, M. Callsen, J. Zhou, J.W. Chai, Y.P. Feng, S.J. Wang, M. Yang. Adv. Mater. Interfaces **6**, 1801160 (2019).
- [48] H. van Gog, W.-F. Li, C. Fang, R.S. Koster, M. Dijkstra, M. van Huis. npj 2D Mater. Appl. **3**, 18 (2019).
- [49] J. Azadmanjiri, P. Kumar, V.K. Srivastava, Z. Sofer. ACS Nano Mater. **3**, 3116 (2020).
- [50] S.K. Radha, K. Crowley, B.A. Holler, X.P.A. Gao, W.R.L. Lambrecht, H. Volkova, M.-H. Berger, E. Pentzer, K.G. Pachuta, A. Schirlioglu. J. Appl. Phys. **129**, 220903 (2021).
- [51] H. Xie, Z. Li, L. Cheng, A.A. Haidry, J. Tao, Y. Xu, K. Xu, J.Z. Ou. iScience **25**, 103598 (2022).
- [52] A.V. Kavokin, M.E. Portnoi, A.A. Varlamov, Y. Yerin. Phys. Rev. B **109**, 235405 (2024).
- [53] Z.Z. Alisultanov, E.G. Idrisov, A.V. Kavokin. Phys. Rev. B **111**, 155430 (2025).
- [54] J.M. Ziman. Principles of the Theory of Solids. Cambridge Univ. Press, Cambridge (1972). Ch. 7.

*Translated by T.Zorina*